

# Static and Dynamic Light Scattering Characterization of Solutions of Hydrophobically Associating Fluorocarbon-Containing Polymers

Thomas A. P. Seery, Maryam Yassini, Thieo E. Hogen-Esch, and Eric J. Amis\*

Department of Chemistry, University of Southern California,  
Los Angeles, California 90089-0482

Received October 25, 1991; Revised Manuscript Received May 12, 1992

**ABSTRACT:** Static and dynamic light scattering measurements have been performed on solutions of a polyacrylamide containing small amounts of the comonomer, 2-(*N*-ethylperfluorooctanesulfonamido)ethyl acrylate. These copolymers demonstrate large viscosity enhancements at concentrations of perfluorinated hydrophobe one-tenth as great as that required for similar enhancements in other hydrophobically or ionomerically associating systems. Light scattering studies of the copolymers show complex behavior indicative of large aggregates even at concentrations as low as 10 ppm. At various concentrations, several diffusive relaxations are observed which are identified with aggregates, single chains, and gel modes. With the addition of surfactant to the solutions, single-chain behavior was observed. A temperature-dependent and  $q$ -independent slow relaxation was also observed in the low-concentration regime.

## Introduction

The unique ability of associating polymer systems to modify solution rheological properties has motivated recent work in this area. Studies of these systems have focused on the large viscosity enhancements obtained at low additive concentration. Investigations of ionomers as additives to nonpolar solutions and studies of hydrophilic chains associating via hydrophobic side groups in aqueous solution have revealed common physical characteristics.<sup>1-5</sup> Recently, Zhang et al. reported<sup>6,7</sup> the preparation of a copolymer of acrylamide and a fluorocarbon-containing acrylate; this copolymer exhibits viscosity enhancements much greater than previously observed. The experiments reported here use static and dynamic light scattering to probe the molecular nature of these polymers in solution so that comparisons to other systems can be made regarding the effects of chain length, spacing of associating moieties, and strength of the associative interaction.

In other systems these types of associations have been shown to involve the formation of micellar domains composed of ionic groups in the case of ionomers in nonpolar solvents and hydrophobic groups in the case of aqueous solutions of hydrophilic chains with hydrophobic side groups. These associations are, in some sense, an intermediate between the transient polymer entanglements found in semidilute solutions and permanent chemical cross-links in covalent gels or networks. In addition to the question of the relative rank of these associations on a scale of interaction strengths, one can also question the distribution of associations between inter- and intramolecular contacts.

Ringsdorf et al. made an indirect observation<sup>4</sup> of micellar structures in associating systems using fluorescent probes sensitive to the microviscosity and local polarity of hydrophobic regions in aqueous solutions. The existence of these micellar microdomains was shown to depend on the type of hydrophobe and on temperature in a range which included the lower critical solution temperature (LCST).<sup>4</sup> Poly(*N*-isopropylacrylamide) (PNIPAM) copolymerized with tetradecyl- and octadecyl-substituted acrylamides demonstrated hydrophobic domain formation

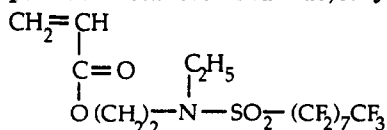
by their fluorescence spectra at polymer concentrations below 0.1%. Copolymers which utilized a decyl-substituted comonomer exhibited no difference in their fluorescence spectra in comparison to the homopolymer, PNIPAM. The hydrophobic domains which were observed below LCST were disrupted by chain collapse above LCST.

Two common difficulties which occur in the synthesis of hydrophilic copolymers that incorporate hydrophobic comonomers arise from the opposite solubility requirements of the monomeric components. The first difficulty is that the hydrophobic comonomer is usually insoluble in the aqueous solvents used in the synthesis of the primarily hydrophilic polymer and, therefore, an organic water-miscible cosolvent is often employed. The second difficulty is to ascertain the degree of comonomer incorporation after synthesis. Schulz and co-workers have addressed both of these problems through the specific design of their comonomer.<sup>5</sup> The hydrophobe of their acrylate comonomer is separated from the ester group by a hydrophilic spacer which solubilizes the comonomer in the reaction bath without cosolvents. The second difficulty is addressed through the inclusion of a phenyl ring in the hydrophobe to allow direct measurement of the comonomer content by ultraviolet spectroscopy. Viscosity enhancements for these polymers were observed at comonomer contents of 0.3 and 0.6 mol %.

Bock and co-workers<sup>1</sup> have enhanced formation of micellar structures by increasing the hydrophilicity of the backbone. Copolymers of acrylamide and various *N*-alkylacrylamides were synthesized and studied at various extents of hydrolysis of the acrylamide backbone. Viscosity data on hydrolyzed chains in aqueous solutions are similar to observations of ionomers in organic solvents where the viscosity is found to be enhanced above the overlap concentration and depressed below the overlap concentration, relative to the parent, hydrolyzed, homopolymer. This behavior is more pronounced at higher hydrophobe levels. Shear thickening is also observed in these solutions but only under fairly limited conditions of solvent, shear rate, polymer concentration, and hydrophobe content. Peiffer has taken a somewhat different approach to increasing the driving force toward hydrophobic association.<sup>8,9</sup> Instead of charging the entire backbone, a charged moiety is placed in the spacer group

\* To whom correspondence should be addressed.

Chart I  
2-(*N*-Ethylperfluorooctanesulfonamido)ethyl Acrylate



which separates the hydrophobe from the main chain. In this way the hydrophobic-hydrophilic differences in the associating unit is enhanced. Peiffer also utilized alkyl-acrylamide comonomers which were prepared with either a quaternary ammonium group or a sulfonate group so that both cationic and anionic modifications could be studied.<sup>8</sup> The importance of hydrophobic associations to the solution properties of these polymers was demonstrated through the effects of added salt and the dependence of hydrophobe chain length. Large viscosity enhancements were also seen in the presence of divalent counterions. The melting points of copolymers with anionic moieties exhibited a minimum with respect to alkyl chain length that was thought to reflect the structure of micellar domains in the bulk.

There are many similarities in the behavior of hydrophobically associating polymers and ionomeric polymers. Initial viscosity measurements on ionomers in nonpolar solvents demonstrated large enhancements of viscosity over that of the parent neutral polymer near the overlap concentration. This feature of the concentration dependence of the viscosity is attributed to network formation via ionic associations. The temperature<sup>10</sup> and solvent dependencies<sup>11,12</sup> of this behavior have been studied extensively. At low concentration the viscosity is observed to decrease relative to uncharged chains of the same degree of polymerization. This feature of ionomer behavior was interpreted as evidence of coil shrinkage due to intramolecular interactions.<sup>11,12</sup>

Recent investigations utilizing neutron scattering have focused on the underlying phenomena in terms of single-chain behavior.<sup>3,13</sup> The most intriguing result of these studies is the observation that lightly sulfonated polystyrene chains ( $\sim 1.0$  % sulfonation) in tetrahydrofuran do not change their dimensions with concentration or with shear rate up to  $1000 \text{ s}^{-1}$ .<sup>3</sup> This study was performed over a concentration range where at low concentration the viscosities of the ionomer solutions were observed to be less than that of the parent polymer and at high concentration the viscosities are higher.

Our study utilizes recently prepared polyacrylamides containing very small amounts (0.7–0.007 mol %) of an acrylate comonomer with the structure shown in Chart I which has a fluorocarbon chain as the hydrophobe. This hydrophobe is expected to exhibit much larger effects than similar hydrocarbon hydrophobes and so to increase the driving force for associations. The concentration of associating groups in our study is between 1 and 2 orders of magnitude lower than that studied in comparable systems utilizing hydrocarbon hydrophobes. Even at such low fractions of hydrophobe, enormous enhancements in solution viscosity have been observed.<sup>6</sup> The viscosity of these substances was previously characterized with regard to temperature, shear rate, concentration of added salt, concentration of added surfactants, and the mole fraction of hydrophobe in the polymer.<sup>6,7</sup>

This study uses light scattering to investigate the underlying molecular behavior responsible for the unique viscosity behavior observed upon variation of the mole fraction of comonomer in the polyacrylamide chains.<sup>6</sup> It is generally difficult to obtain the molecular weight or

radius of gyration of an associating polymer chain due to the omnipresent associations. Our hydrophobes exacerbate this problem as they appear to associate much more strongly than the alkyl hydrophobes studied elsewhere. We have solved this problem by adding surfactants whose hydrophobic ends are also perfluorooctyl groups. These surfactants break up the hydrophobic interactions and allow the observation of single chains. Dynamic light scattering studies of this system over a broad range of polymer concentrations show multiple relaxation times which are consistent with the presence of both inter- and intramolecularly associated polymers. The design of the synthesis did not include an attempt to precisely control either the spacing or the polydispersity of hydrophobes per chain. This randomness, in combination with the inherent molecular polydispersity arising from the radical polymerization, makes the sharpness of the features seen in the data all the more remarkable.

## Experimental Section

**Materials.** Copolymers of acrylamide and a perfluorooctanesulfonamide, FX13 obtained from the 3M Corp., as well as homopolyacrylamide were synthesized following Zhang et al.<sup>6</sup> using standard radical polymerization techniques. The FX13 was purified by recrystallization from methanol. Acrylamide monomer (Polysciences) was an "ultrapure electrophoresis grade" acrylamide which was used as received. Because the samples were being prepared for light scattering studies, attempts were made to reduce dust contamination. The aqueous monomer solutions were filtered into their reaction vessels prior to polymerization using  $0.2\text{-}\mu\text{m}$  nitrocellulose filters (Gelman). The reaction vessels were then covered with rubber septa. Further additions of gases or solutions were delivered via needles inserted through the septa. The reaction solution was purged with argon for 20 min to 1 h prior to addition of an aqueous solution of the initiator, ammonium persulfate. The reaction vessel was magnetically stirred overnight at  $50^\circ\text{C}$ . Previous work<sup>6</sup> has shown that monomer conversion is essentially 100% under these conditions. For this work, four samples synthesized by this procedure were chosen, including one homopolymer and three copolymers. The copolymers were synthesized with 0.007, 0.07, and 0.7 mol % FX13 in the reaction mixtures. Potassium perfluorooctanecarboxylate (FC129), a surfactant whose hydrophobe is sterically equivalent to that of the comonomer, was used in some of the light scattering studies to suppress association of the copolymers.

**Scattering Sample Preparation.** The samples for light scattering were prepared from 4% stock solutions in two series for each polymer sample. The first series of samples, which ranged in concentration from 4% to 0.1% by weight, were diluted with filtered water from the stock solutions which were too viscous to filter. The second series of samples was prepared from an initial stock solution of 0.1% (1000 ppm) concentration. This solution was filtered with  $1.0\text{-}\mu\text{m}$  Nucleopore polycarbonate membrane filters and diluted with filtered water to produce a concentration series ranging from 1000 to 10 ppm. The water used for all dilutions was filtered through  $0.1\text{-}\mu\text{m}$  Nucleopore polycarbonate membranes. In order to test the assumption that the two series did not differ because of their modes of preparation (i.e., equilibrium is attained and concentrations are unaffected by filtering), we also prepared two sets of scattering samples in the range 5000–150 ppm, one filtered, and the other unfiltered.

**Scattering Methods.** Static and dynamic light scattering measurements were made using instrumentation as described previously<sup>14</sup> upgraded to a BI2030AT (Brookhaven Instruments) and controlled by a PC/AT clone. Laser intensities at  $514.5 \text{ nm}$  ranged from 200 to 800 mW, and detector aperture settings were optimized for each set of samples to obtain a photon count rate of  $10^4$ – $10^6$  cps for all concentrations at each molecular weight and temperature. Repeated measurements taken over a period of several months indicated no sample degradation with time.

The weight-average molecular weight,  $M_w$ , the second virial coefficient,  $A_2$ , and the root-mean-squared  $z$ -average radius of gyration,  $R_G$ , were obtained from the static scattering data by

the Zimm plot method. The scattering calibration constants used were as follows: refractive index of water  $n = 1.33$ ; refractive index increment  $(\partial n/\partial c)_{T,p} = 0.165 \text{ mL mg}^{-1}$ ; Rayleigh ratio (for benzene standard)  $R_{90}(\theta) = 2.42 \times 10^{-3} \text{ m}^{-1}$  for  $\lambda = 514.5 \text{ nm}$  and  $25^\circ \text{C}$ .<sup>15</sup>

The  $(\partial n/\partial c)_{T,p}$  for pure polyacrylamide was used in all the static light scattering analyses including measurements made with surfactant added to the solutions. Errors in  $(\partial n/\partial c)_{T,p}$  affect molecular weight determination, and so the validity of this approximation must be addressed. In these experiments, errors can enter from either the polymer or the solvent contributions to  $(\partial n/\partial c)_{T,p}$ . Two solvents, water, and dilute surfactant solutions were used. The addition of up to 1% surfactant did not change the measured solvent refractive index. We can therefore neglect changes in  $n$  for the solvent as a source of error in  $(\partial n/\partial c)_{T,p}$ .<sup>16</sup> The specific refractive index increment of a copolymer can be approximated as the mass weighted average of the specific refractive index increments of its components.<sup>17</sup> In all samples the comonomer constitutes less than 6.0% of the total mass; this makes corrections to  $(\partial n/\partial c)_{T,p}$  due to the incorporation of hydrophobic comonomers into the polyacrylamide chains negligible. A third possibility is that the aggregation process itself may alter  $(\partial n/\partial c)_{T,p}$ . We cannot eliminate this possibility.

Dynamic light scattering data were obtained from the intensity-intensity autocorrelation function of the scattering. Intensity-intensity autocorrelation functions are related to field correlation functions,  $g^{(1)}(\tau)$ , through the Siegert relation:

$$\langle I(0) I(\tau) \rangle = A(1 + \beta |g^{(1)}(\tau)|^2)$$

Field correlation functions derived from systems with multiple modes of relaxation may be represented as the convolution of a relaxation spectrum,  $s(\tau)$ , and an exponential decay:

$$g^{(1)}(\tau) = \int_0^\infty s(\tau) \exp(-t/\tau) dt$$

The correlation functions were deconvoluted using CONTIN, a constrained regularization method by Provencher for inverting Laplace transforms.<sup>18,19</sup> The deconvolution yields the spectrum of relaxation times for the various processes in the scattering sample as a series of amplitudes,  $s(\tau)$ , along a grid of  $\tau$  values. The amplitudes of the modes are indicators of the relative importance of different relaxations. The amplitudes are reported here as a percentage of the total amplitude of  $s(\tau)$ . Apparent hydrodynamic radii were calculated from the relaxation times assuming  $\tau = 1/Dq^2$  and using the Stokes-Einstein relation  $D = kT/6\pi\eta R_h$  with the solvent viscosity  $\eta$ .

## Results

Initial measurements at low concentrations were directed toward establishing a concentration range where single molecule diffusion could be observed for all comonomer levels. Dynamic light scattering data were obtained at a  $40^\circ$  angle for all polymer samples at concentrations ranging over 3 orders of magnitude from 10 to  $10^4$  ppm.

**Homopolymer.** The behavior of the acrylamide homopolymer was investigated first. Static light scattering data, plotted in Figure 1, yield the molecular weight, radius of gyration, and second virial coefficient, listed in Table I. The molecular weight,  $M$ , and radius of gyration,  $R_G$ , are combined to give an overlap concentration,  $c^*$ , of 800 ppm with  $c^* \approx 3M/4\pi R_G^3 N_A$ . Figure 2 shows a correlation function acquired from a 0.2% solution of the polyacrylamide homopolymer in water at  $25^\circ \text{C}$ , which is representative of the data for this polymer above  $c^*$ . The relaxation spectrum is plotted on the same  $\tau$  axis with its amplitude values scaled by  $\tau$  to maintain relative peak areas in different regions of the  $\tau$  axis. Relaxation times are taken to be the average value of a given peak in the spectrum. At high concentrations of homopolymer we see a sharp peak at  $100 \mu\text{s}$  which corresponds to the fast relaxation characteristic of semidilute solutions. The inverse relaxation time shows a  $q^2$  dependence (Figure 3) as is expected for the semidilute pseudo-gel mode.

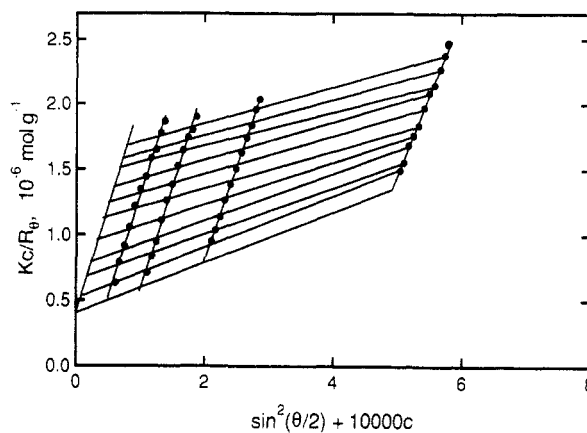


Figure 1. Static light scattering Zimm plot of polyacrylamide homopolymer at  $25^\circ \text{C}$  in water.

Figure 2 also shows several relaxation times in the region from 1 ms to 1 s. Because the correlation function is smoothly decreasing over this range, the three peaks assigned by CONTIN may correspond to the slow mode observed in the semidilute region.<sup>20-22</sup> Several investigators<sup>21,22</sup> have reported a molecular weight scaling of the slow mode of about 2, and if we assume a broad molecular weight distribution in these samples it is reasonable to expect the relaxation times to span several orders of magnitude. The fast mode, on the other hand, has no molecular weight dependence and thus is unaffected by polydispersity so long as all the chains are overlapping. The CONTIN algorithm often represents broad distributions of relaxation times by multiple distinct peaks.<sup>23</sup> Given these considerations, the longer decay time region of the spectrum at these concentrations will be interpreted as simply representing a slow-mode relaxation of semidilute solutions.

At concentrations below  $c^*$ , the correlation functions exhibit a single relaxation. These correlation functions, when analyzed using CONTIN, have a single peak in the resulting spectra. The inverse relaxation time is  $q^2$ -dependent, indicating a diffusive relaxation as expected. Hydrodynamic radii are calculated from the diffusion coefficients and plotted against concentration as solid diamonds in Figure 4. As the concentration approaches  $c^*$  from the dilute region,  $R_h$  decreases slightly, reflecting an increase in  $D$ . The diffusion coefficient can be expressed<sup>24</sup> as a virial expansion in powers of concentration,  $D = D_0(1 + k_D c + \dots)$ , where  $k_D$  is a dynamic virial coefficient and a positive value of  $k_D$  indicates good solvent conditions. Also included in Figure 4 are data from the semidilute region for a fast relaxation and a slow relaxation where both are analyzed as apparent radii. As expected, the curves break near  $c^*$ .

**Copolymer 1.** The copolymer containing 0.007 mol % FX13 gave results that were not strikingly different from the homopolymer. DLS data were obtained at  $40^\circ$  for all concentrations. Relaxation times were extracted using the same procedure as for the homopolymer, and the apparent radii calculated from these relaxation times are plotted against concentration in Figure 4. The results of the static light scattering analysis are presented in Table I. One clear difference between copolymer I and the homopolymer is that their second virial coefficients,  $A_2$ , from the static light scattering reflect different solvent qualities. The homopolymer has a positive  $A_2$  while for the copolymer  $A_2$  is slightly negative, indicating near  $\Theta$  or poor solvent conditions. This observation presumably reflects inter-chain attractions due to the fluorocarbon groups.

Table I  
Light Scattering Results

polymer	MW $\times 10^6$	$R_G$ (nm)	$A_2 \times 10^{-4}$ (mol cm <sup>3</sup> g <sup>-2</sup> )	$R_h(c=0)$ (nm)	$c^*$ (ppm)	dp	hydrophobes per chain	$R_h/R_G$
PAM	2.48	107	9.6	60	802	35K	0	0.56
copolymer 0.007% FX13	1.34	87	-0.078	55	806	19K	1.3	0.63
copolymer 0.07% FX13	6.88	179	3.2	300	475	97K	68	1.67
water/1.0% FC129	6.54	114	2.09	80	1750			0.70
water/0.1% FC129	9.18	143	6.39	70	1244			0.49
copolymer 0.7% FX13	0.75	69	19.5	600	905	11K	74	8.7

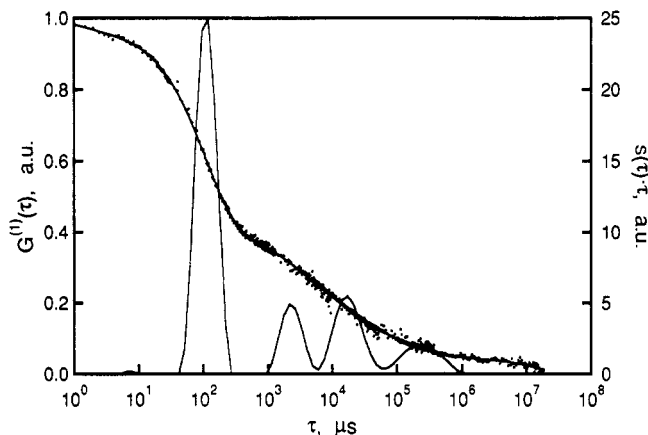


Figure 2. Correlation function and relaxation spectrum from dynamic light scattering data acquired at a 40° angle from a 2000 ppm solution of polyacrylamide in water at 25 °C.

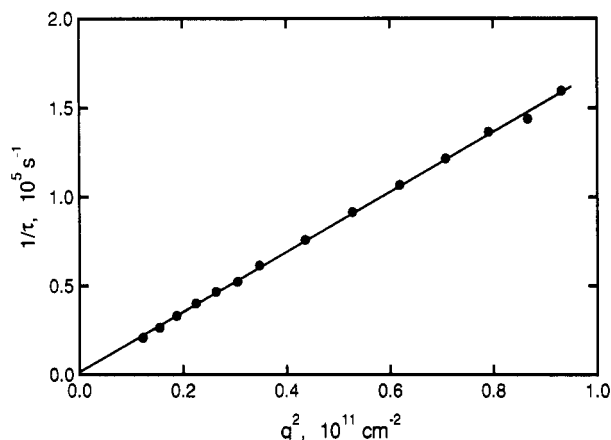


Figure 3.  $1/\tau$  vs  $q^2$  for the pseudo-gel mode of a 2000 ppm solution of polyacrylamide homopolymer at 25 °C in water.

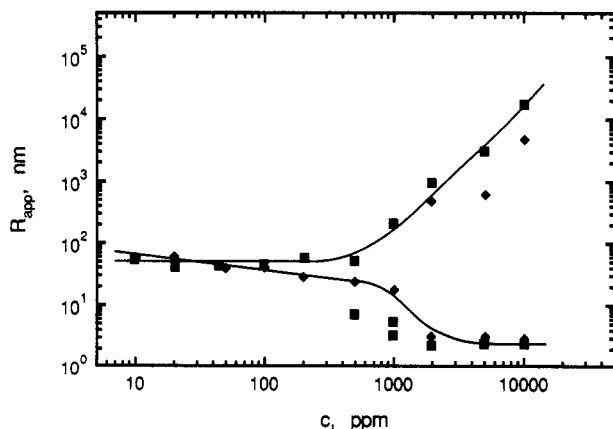


Figure 4. Apparent radius vs concentration for the polyacrylamide homopolymer (◆) and copolymer I (■).

To compare the relative sizes of copolymer I and the homopolymer, we could calculate an expected  $R_G$  from their molecular weights and a molecular weight scaling of  $R_G \sim M^{0.6}$ . From this the expected  $R_G$  is 74 nm instead

of the measured 87 nm for the  $1.34 \times 10^6$  molecular weight copolymer I. Given that the samples are polydisperse and the fact that the measured  $R_G$  is a z-average while  $M$  is a weight-average, these estimates are not too far off. We note that, by using the measured results,  $c^*$  is estimated as 800 ppm for either of these polymers.

The average degree of polymerization (dp) for copolymer I is calculated from the weight-average molecular weight as  $1.9 \times 10^4$  monomers per chain. For 0.007 mol % comonomer (i.e.,  $1.4 \times 10^4$  acrylamide monomers per hydrophobe) there are an average of 1.3 hydrophobes on each chain. Due to these low levels of comonomer, the degree of incorporation could not be measured directly. Previous work<sup>6</sup> found that the acrylamide reacts completely, and preliminary measurements by <sup>19</sup>F NMR monitoring the disappearance of free fluoromonomer indicate quantitative incorporation of the comonomer. If the reactivity ratios are similar, we expect a random distribution of comonomers among the chains. This is reasonable since the reacting double bond of the comonomer is separated from the hydrophobe by a hydrophilic sulfonamide spacer. Previous investigations utilizing acrylamides and alkyl-acrylamides have made similar assumptions.<sup>4,5</sup> Because any micellelike structures in solution would certainly require several hydrophobes, it is unlikely, in this sample, that the requisite number could come from a single chain; therefore, associations in this sample will be primarily intermolecular.

The evidence that the hydrophobic groups perturb this polymer is seen in Figure 4. The apparent radius of the copolymer is constant or slightly increasing (which implies  $k_D \leq 0$ ) as concentration increases through the same dilute region where the homopolymer coils show  $k_D > 0$ . Above the transition to the semidilute regime near 800 ppm in Figure 4, copolymer I behaves very much like the homopolymer. Correlation functions obtained for this polymer at higher concentrations have the same characteristics of semidilute behavior as discussed previously for the homopolymer. The pseudo-gel relaxation is approximately the same for the two polymers. The molecular weight dependent slow mode is slower for the copolymer even though its molecular weight is smaller, which suggests a small amount of aggregation in this region.

**Copolymer II.** The copolymer with 0.07 mol % hydrophobic comonomer is aggregated even at concentrations as low as 10 ppm. Static light scattering data for this polymer in aqueous solution are plotted in Figure 5. The molecular weight, radius of gyration, and second virial coefficient obtained from this analysis are included in Table I. We can estimate the number of hydrophobes per chain by considering that the ratio of FX13 hydrophobe to acrylamide monomer in the reaction bath was 1:1400 and the degree of polymerization of these chains is nearly  $10^5$ . Thus, the average number of hydrophobes per chain is about 70.

Correlation functions for this polymer in aqueous solution exhibit multimodal scattering at all concentrations below 1000 ppm. At the lowest concentrations (10–200

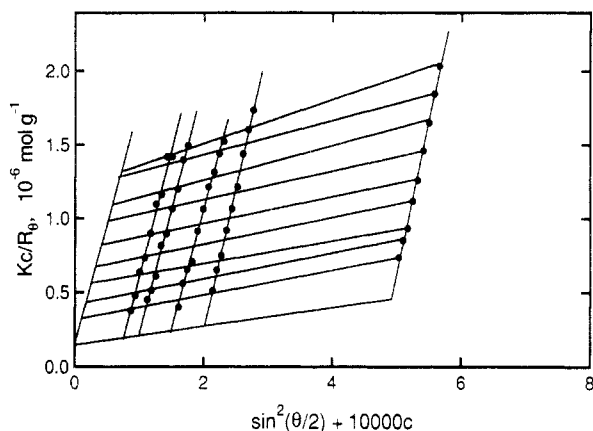


**Figure 5.** Static light scattering Zimm plot of copolymer II at 25 °C in water.

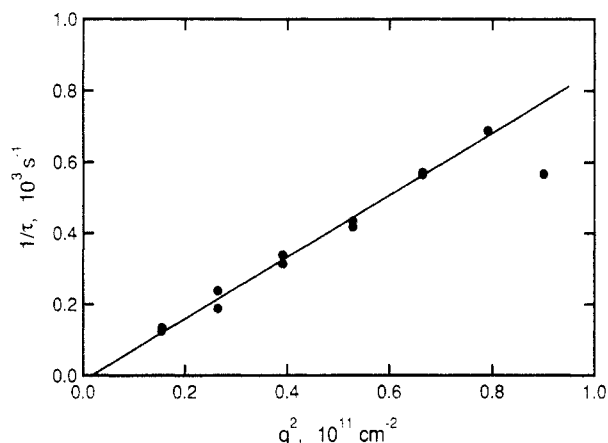


**Figure 6.**  $1/\tau$  vs  $q^2$  for the aggregate mode of a 50 ppm solution of copolymer II at 25 °C in water. The line is a least-squares fit; the diffusion coefficient corresponding to this slope gives a hydrodynamic radius of 315 nm.

ppm) the correlation functions are dominated by a slow relaxation (10 ms to 10 s) whose amplitude is often greater than 50% of the total. This relaxation will be discussed at length below. The next most significant relaxation is  $q^2$  dependent and corresponds to  $R_h$  in the 200–600-nm range for concentrations of 10–200 ppm. Figure 6 shows the  $q^2$  dependence of the inverse relaxation time for a 50 ppm solution of this copolymer. From the diffusion coefficient we obtain an apparent  $R_h$  of 315 nm with the Stokes–Einstein relation. This relaxation reflects diffusion of multichain aggregates formed when the hydrophobes cluster in solution, perhaps as micelles, and thus cause association of the copolymer II chains. The amplitude of this relaxation is nearly 60% of the total at low  $q$  but drops to 33% at 120° scattering angle.

A third scattering mode is also observed for this sample. This relaxation time is also  $q^2$ -dependent (Figure 7), and the amplitude varies linearly with  $q^2$  from 4% to nearly 20% as the angle increases from 45 to 105°.  $R_h$  is calculated from the diffusion coefficient as 36 nm which we identify with chains partially collapsed by intramolecular associations of the hydrophobes. Given an average value of 70 hydrophobes per chain and the implication that the collapsed chains are few because they contribute a small amplitude to the scattering function, we estimate that chain collapse requires more than 70 hydrophobes.

These assumptions as to the sources of the different relaxations are supported by our measurements of the effect of added surfactants. The addition of surfactants in concentrations of 1.0 or 0.1% altered the scattering behavior dramatically. The correlation functions were

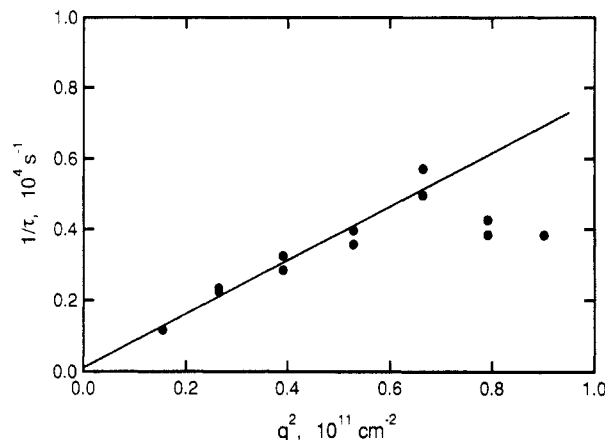


**Figure 7.**  $1/\tau$  vs  $q^2$  for the collapsed coil mode of a 50 ppm solution of copolymer II at 25 °C in water. The line is a least-squares fit; the diffusion coefficient corresponding to this slope gives a hydrodynamic radius of 36 nm. Data at the highest angles were not included in the fit due to poor signal quality.

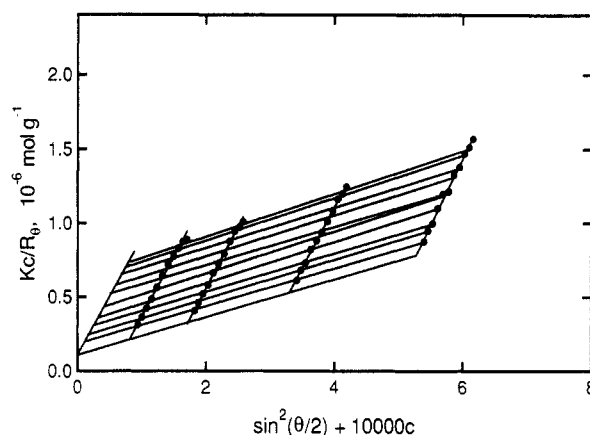


**Figure 8.** Static light scattering Zimm plot of copolymer II at 25 °C in water with 0.1% added FC129.

unimodal at all concentrations below 1000 ppm. The inverse relaxation times from CONTIN were linear in  $q^2$  to give diffusion coefficients corresponding to  $R_h$  between 70 and 80 nm. The absence of other contributions to the scattering indicates that both inter- and intramolecular associations are disrupted to eliminate both aggregates and collapsed chains.

Static light scattering data from the solutions with surfactant were also analyzed, and the results are shown in Table I. Figure 8 shows a Zimm plot of the data for copolymer II in solutions with 0.1% surfactant. The surfactant, FC129, and the comonomer contain sterically equivalent hydrophobic groups. Consequently, there should be no enthalpic barrier to the polymer hydrophobes participating in a micelle composed primarily of surfactant molecules. In the presence of excess surfactant, the hydrophobes can lower their free energy by joining surfactant micelles as opposed to remaining clustered only with other hydrophobes attached to polymers. The abundance and mobility of surfactant relative to comonomer hydrophobes provide a large entropic gain for formation of surfactant micelles.

At concentrations greater than 1000 ppm, aqueous solutions of copolymer II do not exhibit the dynamic behavior characteristic of semidilute solutions. The gel mode is completely absent, and the deconvolutions of the correlation functions now yield a single narrow peak. The relaxation times for these peaks are analyzed as apparent radii and plotted against concentration as filled points in Figure 9 along with the hydrodynamic radii found for the

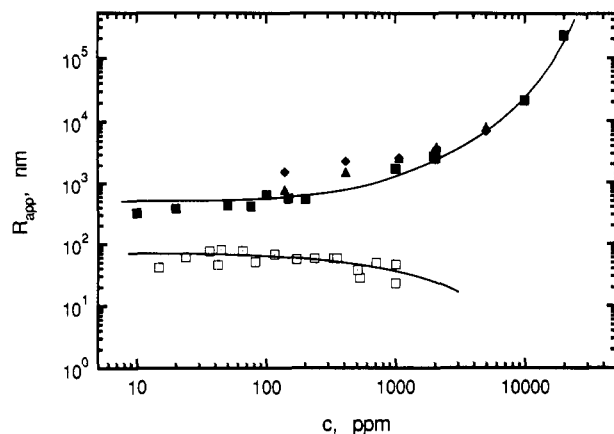


**Figure 9.** Radius vs concentration for aqueous solutions of copolymer II (■) and aqueous solutions prepared to compare preparations with (▲) and without (◆) filtration. The same polymer in the presence of 0.1 (□) and 1.0% (◻) FC129 is shown.

aggregates in dilute solutions without surfactant. These data fall along a smooth curve with no apparent breaks. Solutions prepared with and without filtration over the concentration range 5000–150 ppm were also measured to investigate potential anomalies arising from the initial sample preparation where samples at concentrations above 1000 ppm were not filtered. These new samples showed the same unimodal scattering functions as the first set of samples. Apparent radii calculated from the decay constants for these samples are included in Figure 9 as a function of concentration, and they fit on the same smooth curve as the initial aggregate data. Again, no gel mode was observed.

The absence of dynamic behavior characteristic of semidilute solutions is unusual in this concentration regime, as are the apparent radii in the range 1–200  $\mu\text{m}$ . The chains apparently form increasingly dense structures as they aggregate. As concentration increases, this process continues, and, as newly added chains fill in around the aggregated ones, the volume of the cluster may grow more slowly than its mass. Thus the overlap condition for the semidilute regime is never attained. One mechanism for growth of aggregates in which the solution would remain below  $c^*$  is the combination of clusters so that the number concentration of aggregates would decrease with increasing polymer concentration. This picture of aggregation is supported by neutron scattering studies in the case of ionomers which demonstrated that individual chains do not increase their dimensions upon association<sup>13</sup> as would be expected if the mechanism of aggregation was a transition from intra- to intermolecular association.

Also shown in Figure 9 as open symbols are  $R_h$  values for the same copolymer II solutions with 0.1 and 1.0% surfactant added. As noted, the radii drop to between 70 and 80 nm. A comparison to Figure 4 demonstrates that the data for the solutions with surfactant would match the low concentration data for the homopolymer and for copolymer I (low comonomer content). Furthermore, just as Figure 8 exhibits a positive  $A_2$  for these solutions, Figure 9 is consistent with a positive  $k_D$  similar to the homopolyacrylamide.

**Copolymer III.** The results from the sample with 0.7 mol % of comonomer are quite similar to those of copolymer II. The dynamic light scattering correlation functions showed multiple relaxations at low concentrations and single modes at high concentrations. The relaxation times were analyzed as hydrodynamic radii which are shown plotted against concentration in Figure 10. The slower relaxations at low concentrations corresponded to

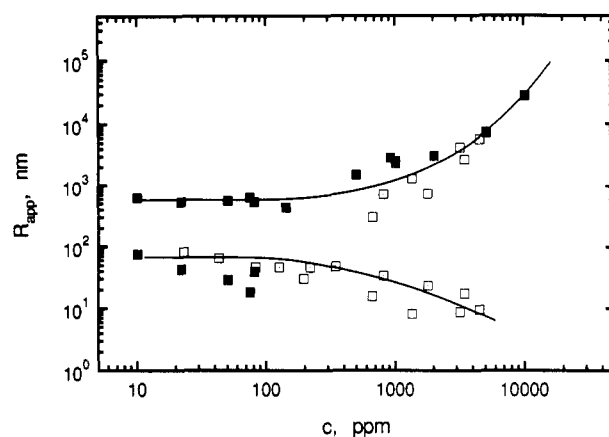


**Figure 10.** Apparent radius vs concentration for copolymer III (■) and for the same polymer in the presence of 0.1 (□) and 1.0% (◻) FC129.

apparent radii of 600 nm. The amplitude of this relaxation varied from 19 to 90% of the total. These aggregates are larger than those for copolymer II and do not show any decrease at the lowest concentrations.

There are also relaxations corresponding to partially collapsed chains. At the lowest concentrations a faster relaxation time can also be extracted from the correlation functions. This relaxation has an amplitude which varies unsystematically from 10 to 78% of the total scattering amplitude. The apparent radius extracted from the faster time constant decreases as the concentration increases from 10 to 100 ppm.

Static light scattering was performed on copolymer III as well. The experiment was hindered by large fluctuations in the scattered intensity which lasted on the order of seconds. Initially this was thought to be dust, and so efforts were made to reject scattering during these fluctuations. Intensity data were acquired in multiple sets (5–6) for each concentration every 5° from 40 to 140°. Intensity values for each angle and concentration were calculated by discarding the high-intensity values at each angle and averaging the remaining values. One source of large intensity fluctuations could be number density fluctuations of the large aggregates seen in the dynamic light scattering, and this method of discriminating against dust in the static intensities would bias the results toward lower values of molecular weight and radius of gyration. The results from the analysis of this static data are included in Table I for completeness but must be considered in light of the above caveat. In particular, we believe the true molecular weight and  $R_G$  to be considerably higher.

Despite the high comonomer content of copolymer III, associations were inhibited by added surfactant. Again, at low concentrations, the samples with surfactant exhibit single relaxations corresponding to hydrodynamic radii of 40–80 nm which are characteristic of single-chain dimensions. These radii are plotted against concentration in Figure 10 along with data for the corresponding solutions without surfactant. The breaking of intermolecular associations by the surfactant is seen from our lowest polymer concentrations up to 500 ppm. Above 500 ppm the 0.7% sample shows two relaxations, one of which is qualitatively similar to the pseudo-gel relaxation observed at high concentrations of the homopolymer or copolymer I. This fast relaxation is narrowly distributed and corresponds to a hydrodynamic radius on the order of 10 nm. The slower relaxation is narrower than the slow semidilute relaxation seen for the homopolymer. The concentration dependence of these apparent radii, in the presence of surfactants, is similar to that seen for homopolymer and



copolymer I (Figure 4) and qualitatively different from those seen in aqueous solutions without surfactant.

### Discussion

Interpretation of the static light scattering with added surfactant may be complicated by preferential solvation of copolymer segments. The molecular weight of polymer with associated surfactant should be larger than that of the polymer alone, and the scattering power of the system may be affected as well. Because we observe a decrease in the apparent molecular weight as more surfactant (up to 1.0%) is added, we suspect that these are not serious complications. Furthermore, our conclusion that surfactants reduce the hydrophobic associations of the copolymers is supported by the decrease of molecular weight and  $R_G$  at higher surfactant concentration.

Another aspect of this system to be considered is the change in coil density between the aggregated and the single-chain state. The ratio  $R_h/R_G$  can be used as a measure of the density of polymeric structures.<sup>25</sup> In the aggregated case this ratio is 1.7, while after addition of surfactant it drops to 0.5. These values can be compared to a dense, highly branched poly(vinyl acetate) microgel,<sup>25</sup> which gives a value of 2.0, and a random coil, which gives a value of 0.5.

The measured radii of gyration are independent of parameters such as  $(\partial n/\partial c)_{T,p}$  which affect the absolute molecular weight determination. The  $R_G$  for copolymer II in pure water is 179 nm but, in solutions containing FC129,  $R_G$  is 143 nm with 0.1% FC129 and 114 nm with 1.0% FC129. At the least this is consistent with a deaggregation process expected in the presence of surfactants that solubilize the hydrophobes. The change in  $R_h$  from 200 to 70 nm for copolymer II and the 10-fold decrease in  $R_h$  for copolymer III in the presence of surfactants are more dramatic evidence of the fact that aggregates are broken down. The difference in the magnitude of changes in  $R_G$  and  $R_h$  further reflects the changing coil density as discussed above.

Although the magnitude of the second virial coefficient,  $A_2$  is subject to the same errors as the molecular weight, the sign of  $A_2$  is a robust feature of the data. In Table I we show that water is a good solvent for the homopolymer but that copolymer I is near its  $\Theta$  condition. On the other hand, as the amount of comonomer is increased to 0.07 or 0.7 mol %,  $A_2$  increases, suggesting that we are again in a good solvent regime. This may at first seem counter-intuitive but may be understood as suggesting that the hydrophobes of a given chain gather into a micelle surrounded by the chain backbone which extends into the solution. This chain, like the homopolymer is in good solvent and demonstrates excluded-volume interactions with other clusters. Thus, while intramolecular interactions are attractive and intermolecular interactions draw chains together to aggregate, the aggregates themselves show a positive  $A_2$  value. The fact that stable clusters of reasonably well-defined size form over the broad low concentration range without phase separation further reinforces that  $A_2$  is not becoming negative. The possibility of separating  $A_2$  values into intra- or interchain excluded-volume effects has also been proposed.<sup>26</sup>

The  $q^2$  dependence of the diffusive relaxations should be sensitive to the change in density between the aggregates and the chains with added surfactant. Figure 6 is  $1/\tau$  for the aggregate diffusion plotted against  $q^2$ . It is unusual to see a completely linear relation for this plot when  $qR_h$  is in the range 0.8–6.2, as is the case for this plot. In contrast, Figure 11 shows  $1/\tau$  vs  $q^2$  for the much smaller radius species measured in the presence of added sur-

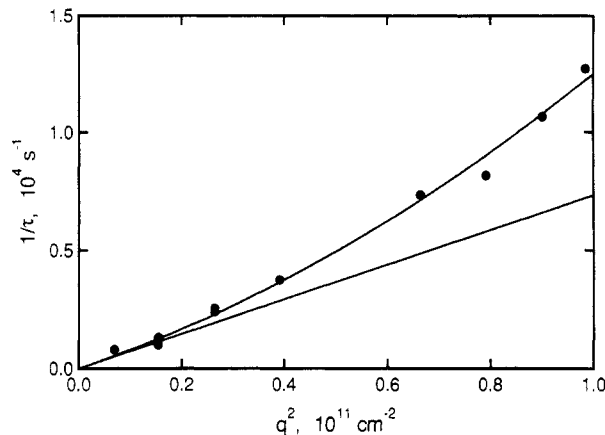


**Figure 11.**  $1/\tau$  vs  $q^2$  for a 200 ppm solution of copolymer III at 25 °C in water with 0.1% added FC129. The curve is fit as described in the text; the line corresponds to limiting slope as  $q^2 \rightarrow 0$ .

factant. In this case there is noticeable curvature of the plot. We have taken the  $R_h$  as the limiting slope of  $1/\tau$  vs  $q^2$  as  $q^2 \rightarrow 0$ . Burchard<sup>25</sup> showed that the curvature in a plot of  $1/\tau$  against  $q^2$  is related to  $R_G$  by the equation

$$1/\tau q^2 = D_0(1 + C(q^2 R_G^2))$$

where  $C$  is a constant that increases weakly with increasing polydispersity and decreases strongly with increasing density or branching. The difference between Figures 6 and 11 may be explained in terms of the chain density. In the surfactant solution the aggregated chains are no longer held tightly together by the hydrophobic associations and thus adopt an open random-coil configuration as in a good solvent. If we use the good solvent value<sup>25</sup> of  $C = 0.2$  to fit the data shown in Figure 11 with the quadratic form shown above, we calculate  $R_G$  of 37 nm. This is in reasonable agreement with the  $R_h$  of 29 nm found at this concentration.

In the course of studying the diffusive modes we found a much slower mode which dominated the spectrum of relaxations at low concentrations. Initially this was assumed to be the result of contamination, but it persisted in all samples despite extensive filtration efforts. The slow relaxation occurred at experimentally accessible correlation times for copolymer II at low concentrations and may have occurred for higher concentrations or other samples at delay times outside the dynamic range of our correlator. The observed modes had time constants ranging from 50 ms to 7 s and were dependent upon concentration and temperature. Figure 12 shows the relaxation times for three different temperature-concentration combinations against  $q^2$ . Clearly the relaxations are independent of angle and therefore not related to diffusion. From the order of magnitude difference between the relaxation time of the 100 ppm sample at 30 °C and the same sample at 60 °C we see a strong temperature dependence. The strong dependence on concentration is also obvious in the data for the 20 ppm sample at 25 °C. A similar slow mode has been noted in solutions of associating ionomers,<sup>27</sup> it may be related to the activation barrier for a "sticker" to migrate from one hydrophobic region to another. Further investigation of this relaxation is continuing using a correlator with an extended dynamic range.

### Conclusions

Static and dynamic light scattering experiments performed on solutions of hydrophobically associating polyacrylamide copolymers illuminate the underlying molec-

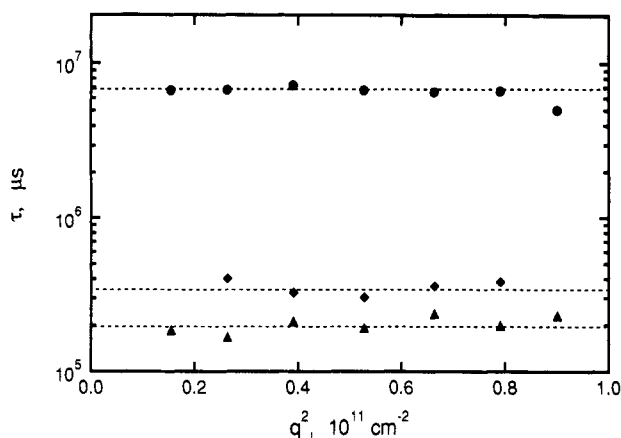


Figure 12.  $\tau$  vs  $q^2$  for copolymer II, 100 ppm at 30 °C (●), 100 ppm at 60 °C (▲), and 20 ppm at 25 °C (◆), in water.

ular basis for previous viscosity measurements. Aggregation effects for these polymers are observed at polymer concentrations as low as 10 ppm. These effects are manifest by large radii of multichain aggregates as well as small radii attributed to collapsed chains. The aggregates are denser than random coils and are comparable to microparticle clusters observed in other systems. Addition of surfactant breaks up the associations and produces chains with less dense structures that reflect random-coil configurations. A very slow temperature- and concentration-dependent relaxation is also found which is independent of the scattering vector. Further studies of these solutions are necessary to understand the origin of this relaxation mode.

**Acknowledgment.** Helpful discussions with Professor Y. Rabin concerning interpretation of the experimental results are gratefully acknowledged. This work was supported by the U.S. Department of Energy—Materials Sciences (DE-FG03-89ER45407). Support from a U.S. Department of Education Fellowship Grant to the USC Department of Chemistry (T.A.P.S.) is also gratefully acknowledged.

## References and Notes

- (1) Bock, J.; Siano, D. B.; Valint, P. L., Jr.; Pace, S. J. In *Polymers in Aqueous Media*; Glass, J. E., Ed.; American Chemical Society: Washington, DC 1989; p 570.
- (2) Lantman, C. W.; MacKnight, W. J.; Peiffer, D. G.; Sinha, S. K.; Lundberg, R. D. *Macromolecules* **1987**, *20*, 1096.
- (3) Pedley, A. M.; Higgins, J. S.; Peiffer, D. G.; Rennie, A. R.; Staples, E. *Polym. Commun.* **1989**, *30*, 162.
- (4) Ringsdorf, H.; Venzmer, J.; Winnik, F. M. *Macromolecules* **1991**, *24*, 1678.
- (5) Schulz, D. N.; Kaladas, J. J.; Maurer, J. J.; Bock, J.; Pace, S. J.; Schulz, W. W. *Polymer* **1987**, *28*, 2110.
- (6) Zhang, Y.-X.; Da, A.-H.; Hogen-Esch, T. E.; Butler, G. B. *J. Polym. Sci., Polym. Lett. Ed.* **1990**, *28*, 213.
- (7) Zhang, Y.-X.; Da, A.-H.; Hogen-Esch, T. E.; Butler, G. B. *Polym. Prepr. (Am. Chem. Soc., Div. Polym. Chem.)* **1990**, *30*, 338.
- (8) Peiffer, D. G. *Polymer* **1990**, *31*, 2353.
- (9) Peiffer, D. G. *Polymer* **1991**, *32*, 134.
- (10) Lundberg, R. D.; Makowski, H. S. *J. Polym. Sci., Polym. Phys. Ed.* **1980**, *18*, 1821.
- (11) Agarwal, P. K.; Garner, R. T.; Graessley, W. W. *J. Polym. Sci., Polym. Phys. Ed.* **1987**, *25*, 2095.
- (12) Lundberg, R. D.; Phillips, R. R. *J. Polym. Sci., Polym. Phys. Ed.* **1982**, *20*, 1143.
- (13) Gabrys, B.; Higgins, J. S.; Lantman, C. W.; MacKnight, W. J.; Pedley, A. M.; Peiffer, D. G.; Rennie, A. R. *Macromolecules* **1989**, *22*, 3746.
- (14) Seery, T. A. P.; Shorter, J. A.; Amis, E. J. *Polymer* **1989**, *30*, 1197.
- (15) Moreels, E.; De Ceuninck, W.; Finsy, R. *J. Chem. Phys.* **1987**, *86*, 618.
- (16) Arichi, S.; Yoshida, Y.; Ogawa, Y. *Bull. Chem. Soc. Jpn.* **1975**, *48*, 1417.
- (17) Benoit, H.; Froelich, D. In *Light Scattering from Polymer Solutions*; Huglin, M. B., Ed.; Academic Press: New York, 1972.
- (18) Provencher, S. W. *Comput. Phys. Commun.* **1982**, *27*, 213.
- (19) Provencher, S. W. *Comput. Phys. Commun.* **1982**, *27*, 229.
- (20) Stepanek, P.; Jakes, J.; Konak, C.; Johnsen, R.; Brown, W. *Polym. Bull.* **1987**, *18*, 175.
- (21) Amis, E. J.; Han, C. C.; Matsushita, Y. *Polymer* **1984**, *25*, 650.
- (22) Brown, W. *Macromolecules* **1984**, *17*, 66.
- (23) Jakes, J. *Czech. J. Phys. B* **1988**, *38*, 1305.
- (24) Schaefer, D. W.; Han, C. C. In *Dynamic Light Scattering, Applications of Photon Correlation Spectroscopy*; Pecora, R., Ed.; Plenum Press: New York, 1985; p 420.
- (25) Burchard, W. *Adv. Polym. Sci.* **1983**, *48*, 1.
- (26) Dondos, A.; Tsitsilianis, C.; Staikos, G. *Polymer* **1989**, *30*, 1690.
- (27) Higgins, J., personal communication.